International Journal of Computational Methods and Experimental Measurements
Vol. 11, No. 2, June, 2023, pp. 73-78
Journal homepage: http://iieta.org/journals/ijcmem

# Investigation of the Fatigue Strength Behaviour of a Fine 2 mm Module Gear

Franco Concli*, Lorenzo Fraccaroli

Libera Università di Bolzano/Bozen, Piazza Università, Bolzano 39100, Italy

Corresponding Author Email: franco.concli@unibz.it

https://doi.org/10.18280/ijcmem.110202

**Received:** 8 June 2022
**Accepted:** 12 April 2023

***Keywords:***
*gears, STBF, 39NiCrMo3, fatigue*

**ABSTRACT**

Gears are among the most widespread mechanical component. Thanks to new technologies, new production methods and new materials on the market, the use of this component is constantly increasing. This fact outlines the need to understand properly the functioning of such component into different load cases. Nowadays the trend of miniaturization is growing in the mechanical sector and gears that have reduced its size are already used in several fields. This fact brings the necessity to correct analyze and study material properties and the fatigue behavior of this mechanical component. Failures resulting from cyclic stress, thus due to fatigue, must be correctly analyzed. This important aspect reduces the life of a generic component by causing unexpected breaks. For this purpose, in the present manuscript, a combined approach of theoretical calculation and experimental analysis is presented, the aim was to investigate the fatigue comportment of a gear made by 39NiCrMo3 with a fine module $m_n$ equal to 2. Single Tooth Bending Fatigue (STBF) tests were realized with the support of a universal tensile testing machine. New grips have been developed for performing fatigue tests on the tensile test machine and, moreover, dimensions of the new grippers were chosen in order to exploit the Wildhaber W5 property. The fatigue limit was approximated thanks to two different statistic approaches, the classic and the shortest stair-case method proposed by Dixon. Both analyses allow to compute the fatigue limit by performing tests at different loads. The step load used in this research was set at $\Delta F = 100N$. The Dixon approach allows to use few tests with respect to the classic method, reducing time and material needed for the analyses. Furthermore, by using the standard ISO 6336 it is possible to translate the applied forces into stress values. Afterward, results of the combined theoretical/experimental analyses were related to the one proposed by the ISO standard of the same steel constituent.

## 1. INTRODUCTION

Miniaturization is a trend is in a steep rise in every engineering field, so as the use of small mechanical components. In fact, the use of small gears that have a module $m_n$ equal or less than 2 is always more present. Gears have a lot of different applications i.e., power transmission, automation, and manufacturing processes, only to mention some of the most relevant. It was also studied that if small sized gears are used it is possible to reduce the pollutant constituents emitted in the atmosphere [1]. This brings to the necessity to properly study and analyze gears constituents, in particular their mechanical behavior. The objective of this framework was to give importance to the phases that are used for calculating constituent's characteristic, precisely, the admissible root tooth bending stress $\sigma_{Flim}$, and to evaluate results for the tested steel (39NiCrMo3). Commonly, the procedure for the design phase of gears is governed by the following standards, ANSI/AGMA 2001-D04 [2], the EU ISO 6336 [3] and the DIN 3990 [4]. Nevertheless, these approaches are founded on studies performed on gears with a module $m_n$ equal to 5. In fact, big sized gears ($m_n \geq 5$) were already investigated by the study [5-9] and moreover, these researches have brought out that the actual standards developed for gears have the trend to overestimate the fatigue strength of the component. More deeply, it was highlighted that the solution is hugely influenced by the size of the gear. In regard to the tooth root bending capacity, in a study carried out by Steutzger [10], it was reported that if gears having a nominal module $m_n \geq 5$ are used, it is possible to observe an incorrect computation of gears parameters. This fact was also confirmed by other researchers [11-13]. Big module nitrited and carburized gears and their tooth root bending behavior was the objective of past researches [14-16].

The comportment of gears during operation is affected by numerous aspects i.e., the surface obtained during machining operation, the heat treatment applied on the final component, the effective geometry of the gear and the temperature in which it is working, just to mention the most important. In the past years some researches on gears with normal module $m_n$<5 have been carried out by the study [17, 18]. Nevertheless, in order to have more reliable data for designing gears, more efforts should be put in the study of small sized gears. In this work the ISO 6336 method B was followed. This standard is based on the evaluation of two key parameters, specifically two stresses are compared. The first is called permissible stress $\sigma_{FP}$, that is computed according to Eq. (1), and the second one is called effective stress $\sigma_F$ that is the stress that is acting on the tooth computed as Eq. (2).

$$\sigma_{F0} = \frac{F_t}{b \cdot m} \cdot Y_F \cdot Y_S \cdot Y_\beta \cdot Y_B \cdot Y_{DT} \tag{1}$$

$$\sigma_F = \sigma_{F0} \cdot K_A \cdot K_V \cdot K_{F\beta} \cdot K_{F\alpha} \tag{2}$$

In Eq. (3) it is possible to see the simplified formulation for the effective stress $\sigma_F$. According to the use and the geometry of the inspected gear to the correction coefficients $Y_\beta$, $Y_{DT}$ and $Y_B$ were assigned a unitary value.

$$\sigma_F = \frac{F_t}{b \cdot m} \cdot Y_F \cdot Y_S \cdot K_A \cdot K_V \cdot K_{F\beta} \cdot K_{F\alpha} \tag{3}$$

In Eqns. (4) and (5) are described respectively the form factor $Y_F$ (Figure 1) and the stress correction factor $Y_S$.

$$Y_F = \frac{\frac{6h_{Fe}}{m} \cdot cos\alpha_{Fen}}{\left(\frac{S_{Fn}}{m_n}\right)^2 \cdot cos\alpha_n} \tag{4}$$

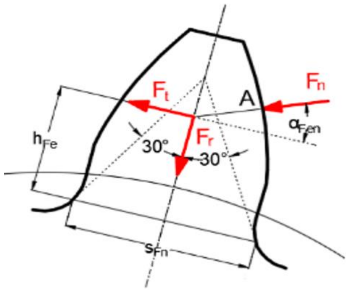


**Figure 1.** Schematic representation of data needed for computing the form factor $Y_F$

$$Y_s = (1.2 + 0.13 \cdot L) \cdot q_s^{\frac{1}{1.21+\frac{2.3}{L}}} \tag{5}$$

With $L$ described through Eq. (6) and the notch sensitivity $q_s$ defined following Eq. (7):

$$L = \frac{s_{Fn}}{h_{fe}} \tag{6}$$

$$q_s = \frac{s_{Fn}}{2 \cdot \rho_F} \tag{7}$$

The application factor $K_A$ is strongly dependent on the application in which the gear is used because it takes into account effects caused by external loads. The dynamic factor $K_V$ has a high dependency on internal dynamics loads. Moving to $K_{F\alpha}$ and $K_{F\beta}$ it is possible to say that they are necessary to manage uneven and transverse loads that act on gears while contact occurs. The deflection of the component and defects arising from machining operation can determine the above-mentioned phenomena.

Following the international standard [3], it is possible to compute and connect $\sigma_{FP}$ with $\sigma_F$. In other words, following the method B of the standard it is possible to relate the allowable stress with the effective one, this relation is written as Eq. (8):

$$\sigma_{FP} = \sigma_{Flim} \cdot Y_{ST} \cdot Y_{NT} \cdot Y_{\delta relT} \cdot Y_{RrelT} \cdot Y_X \tag{8}$$

By comparing Eq. (8) and Eq. (3) it is possible to compute $\sigma_{Flim}$ with Eq. (9).

$$\sigma_{Flim} = \frac{Ft}{b \cdot m} \cdot \frac{Y_F \cdot Y_S}{Y_{ST} \cdot Y_{NT} \cdot Y_{\delta relT} \cdot Y_{RrelT} \cdot Y_X} \tag{9}$$

$Y_{ST}$ and $Y_{NT}$ are respectively the stress and the life factors. $Y_{\delta relT}$ takes into account the notch while $Y_{RrelT}$ the surface of the component. Another important factor that needs to be under review is the size factor $Y_X$. This coefficient, besides considering the effective dimension of the gear, evaluates how stress gradients, weak points, presence of defects etc. [3] are influenced by the size of the gear. The standard ISO 6336 method B states that the coefficient $Y_X$ is unity if a gear with module $m_n$<5 is considered. This assumption may lead to an overestimation of the size of the gear. In this regard another approach for evaluating the size factor $Y_X$ has been proposed by Dobler et al. [19], this method is suited for gears that have a fine module. The Dobler equation representing the size factor is shown in Eq. (10):

$$Y_{XDobl} = 1 - 0.45 \cdot log\left(\frac{m_n}{5}\right) \pm 0.075 \tag{10}$$

According to literatures [20, 21], an additional correction factor must be used for translating results of the STBF tests into results that can be compared with the one obtained with classic meshing gear test. This factor takes into account the different load history between the two types of tests. As main objective this work wants to calculate the fatigue limit (STBF) of the material and to evaluate its comportment when subjected to cyclic loads. Above all, the International standard ISO 6336 method B in combination with the Dobler et al. approach for computing the size factor were used. For the computation of the fatigue limit two similar statistic approaches were used. Both of them relies on statistics, the main difference is the number of samples needed for the correct computation of the fatigue limit. For the first approach, the classic one, a big amount of specimen is required. This method can lead to more reasonable results at the expense of the time and cost required to carry out the tests. The short stair case approach developed for small samples [22] permits to calculate the fatigue limit by means of less than six tests. The use of the last-mentioned method permits to accelerate the testing procedure. Both methods are commonly used for the computation of the fatigue limit for different materials [23, 24]. The secondary purpose of the work was to evaluate and compare the results achieved with two different statistic methods.

## 2. MATERIAL AND METHODS

**Table 1.** Geometrical data of the tested gear

| **Nominal Module ($m_n$)** | 2.00 [mm] |
|---|---|
| **N. of teeth ($z$)** | 26 [-] |
| **Normal pressure angle ($\alpha_n$)** | 20 [°] |
| **Face width ($b$)** | 20.00 [mm] |
| **Profile shift coefficient ($x$)** | 0.30 [-] |
| **Dedendum coefficient ($h^*_{Fp}$)** | 1.25 [-] |
| **Addendum coefficient ($h^*_{ap}$)** | 1.00 [-] |
| **Root radius factor ($\rho^*_{Fp}$)** | 0.38 [-] |
| **Wildhaber ($w$)** | 5 [-] |
| **Formal correction factor ($Y_F$)** | 2.02 |
| **Stress correction factor ($Y_S$)** | 1.90 |

For calculating the limit stress value $\sigma_{Flim}$ associated to the tooth root experimental tests were performed. Specifically, STBF test were performed on a fine module ($m_n$=2) gear made of 39NiCrMo3. In this analysis the tested gears were not thermally treated, the measured hardness was 369 HV. The main characteristic of the gear inspected are shown in Table 1. Data necessary for the calculation of coefficients mentioned in the above paragraph were extrapolated from 2D cad drawings of the inspected geometry.

Single tooth bending fatigue Tests were done on a universal tensile test machine, specifically the STEPlab UD 04 [25]. This machine was able to apply a maximum load of 5KN and, moreover, it features that permits to apply pulsatory loads at a 35Hz rate was used. In order to mount the gear on the machine, custom attachments have been specifically designed (see Figure 2). Thanks to these new grippers it was possible to perform more than one test on a single gear sample by simply rotating the gear for the different load levels. They are rated to withstand the maximum forces that the machine can output and can be directly clamped on the machine.

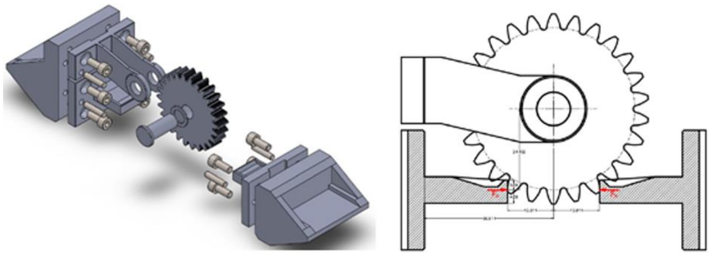

**Figure 2.** On the left 3D drawing of the custom gripper developed by authors. On the right a 2D sketch of the mounted gear

In Figure 3 it is shown the experimental setup used. The correct gear positioning was ensured thanks to a central pin that was used during the placement of the specimen and removed before the test. How demonstrated in [15, 26, 27], to reduce movements of the gear and to keep the specimen in the correct position during the test, a constant load ratio of $R$=0.1 was applied. Once the initial load was applied, and the pin removed it was possible to proceed with the real test.

**Figure 3.** Dedicated machine tool with the gear positioned between anvils

Considering the geometry of the inspected gear a Wildhaber $W$5 was set. It is possible to describe the Wildhaber distance as how many teeth are within anvils during tests. This property depends on the geometrical characteristic of the tested gear. The correct definition of this distance ensures the correct application of forces during test run. For the estimation of the single tooth bending fatigue limit, two different stair-case approaches were used, the classic and the shorter one. Both rely on statistics and permit, through different methods, to compute the fatigue limit. Commonly, a diverse load is applied to each experimental test. More precisely, a load step $\Delta F$ was set, the choice of this force increment may lead to different results, in fact it must be chosen considering several aspects. A reduced increment of $\Delta F$ is going to improve the precision, but on the other hand, it requires a high number of tests. Generally, the increment should not exceed the standard deviation of the data distribution.

Starting from the short staircase procedure, it can be described by $F_{i+1} = F_i \pm \Delta F$. The first test is done at a force level of $F_i$. The second test $F_{1+i}$ is done at a new force level that depends on the outcome of the previous test. It has to be noticed that the RO (Run-Out) condition was set at five million cycles. For the estimation of the fatigue limit the first failure is considered (short staircase approach), or in other words, the force value associated at that rupture is considered (Eq. (11)). The parameter $k$ can be defined through statistic following the tests history. In particular, the Run out (RO) – Failure (F) sequence is taken into account.

$$F_{FP_{STBF50\%}} = F_1 + k \cdot \Delta F \tag{11}$$

The classic method follows the same test procedure of the above mentioned one, namely tests are performed at different levels of load according to their fail-run out condition. In this case the fatigue limit is computed considering equation 12. $F_{FP}$ is the force associated to the fatigue limit, $n$ is the number of total tests performed, $l$ is the number of force levels used, $v_j$ is the number of times in which a defined stress level is repeated and $F_j$ is the associated force to that level.

$$F_{FP} = \frac{1}{n}\sum_{j=1}^{l} v_j F_j \tag{12}$$

## 3. RESULTS

Results of the experimental STBF tests with the short staircase and classic approaches are shown in Table 2 and Table 3 respectively. For computing all the correction coefficient, dimensions were taken from the related CAD model. The standard deviation of the distribution is approximatively $\sigma$=64$N$ for the shorter method, thus lower than the increment applied.

The first step to calculate the tangential force $F_t$ is to multiply the used forces by the pressure angle $\alpha_{Fen}$ (see Figure 1). The factor $k$ was set equal to $k$=−0.296. Thus, thanks to Eq. (9) the value of force with a 50% failure likelihood was set as $F_{FP_{STBF_{50\%}}} = 3071.6\ N$. The results of the short staircase method are shown in Figure 4.

**Table 2.** Results of the short staircase approach

| Test | $Fn_{min}[N]$ | $Fn_{max}[N]$ | $N\ [-]$ | Status |
|---|---|---|---|---|
| **1** | $-395$ | $-3950$ | 3330753 | F |
| **2** | $-385$ | $-3850$ | $5e10^6$ | RO |
| **3** | $-395$ | $-3950$ | $5e10^6$ | RO |
| **4** | $-405$ | $-4050$ | 417250 | F |
| **5** | $-395$ | $-3950$ | $5e10^6$ | RO |
| **6** | $-405$ | $-4050$ | $5e10^6$ | RO |

**Table 3.** Results of the classic staircase approach

| Test | $Fn_{min}[N]$ | $Fn_{max}[N]$ | $N\ [-]$ | Status |
|---|---|---|---|---|
| **1** | $-385$ | $-3850$ | 900234 | F |
| **2** | $-375$ | $-3750$ | 1345870 | F |
| **3** | $-365$ | $-3650$ | $5e10^6$ | RO |
| **4** | $-375$ | $-3750$ | 1243564 | F |
| **5** | $-365$ | $-3650$ | 1856020 | F |
| **6** | $-355$ | $-3550$ | 2456823 | F |
| **7** | $-345$ | $-3450$ | $5e10^6$ | RO |
| **8** | $-355$ | $-3550$ | 2014538 | F |
| **9** | $-345$ | $-3450$ | $5e10^6$ | RO |
| **10** | $-355$ | $-3550$ | 2245683 | F |
| **11** | $-345$ | $-3450$ | 2956327 | F |
| **12** | $-335$ | $-3350$ | $5e10^6$ | RO |
| **13** | $-345$ | $-3450$ | 3156740 | F |
| **14** | $-335$ | $-3350$ | $5e10^6$ | RO |
| **15** | $-345$ | $-3450$ | 3456724 | F |
| **16** | $-335$ | $-3350$ | $5e10^6$ | RO |

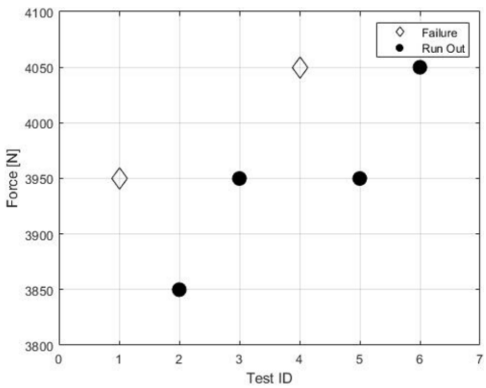


**Figure 4.** Short stair-case results

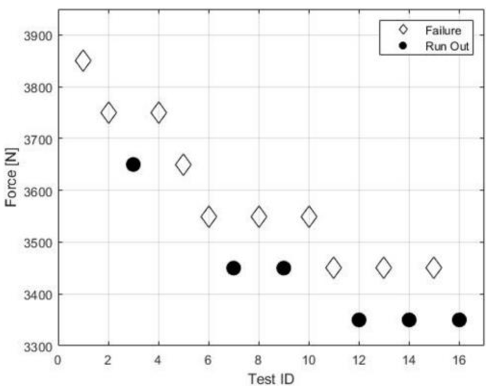


**Figure 5.** Classic staircase results

By applying the standard staircase, 16 specimens were tested at different load levels. Results are presented in Figure 5. In this case the standard deviation was found at $\sigma$=154$N$ that is above the increment of 100N applied. Tests were performed on new sample gears.

By following the equations in the previous paragraphs, it was possible to compute the related stresses acting on the root tooth flank $\sigma_{F2mm}$=658.47 $MPa$ for the short case and $\sigma^*_{F2mm} = 676.25\ MPa$ for the classic approach. According to literature [20, 21] this value needs to be modified since tests were not done on real meshing gears, therefore another correction factor equal to 0.9 was used. At this point the effective root tooth bending stress was calculated at $\sigma_{F2mm}$=592.63 $MPa$ and $\sigma^*_{F2mm} = 608.62MPa$ respectively for the short and classic methods. For the computation of all the other correction coefficients, needed for the calculation of $\sigma_{FP}$, the following considerations were taken. In this specific case the stress factor of the tested gear $Y_{ST}$ was set $Y_{ST}$=2 and the life factor $Y_{NT}$ equal to 1. A roughness $R_a$=6.3$\mu m$ was measured experimentally. This value can now be translated into $R_z$ thanks to the DIN 4778 [28]. Following the standard ISO 6336 the value of $Y_{RrelT}$ related to this roughness value $R_z$ =38.3$\mu m$ is $Y_{RrelT} = 0.9458$. Considering Eq. (13) it was also possible to calculate the notch sensitivity factor $Y_{\delta relT}$, obtaining a value of $Y_{\delta relT}$ =0.9475. $X^*$ is the relative stress gradient and $\rho'$ the slip-layer thickness (the method for calculating those values is described in [3, 29] respectively).

$$Y_{\delta relT} = \frac{1+\sqrt{\rho' \cdot X^*}}{1+\sqrt{\rho' \cdot X^*_T}} \tag{13}$$

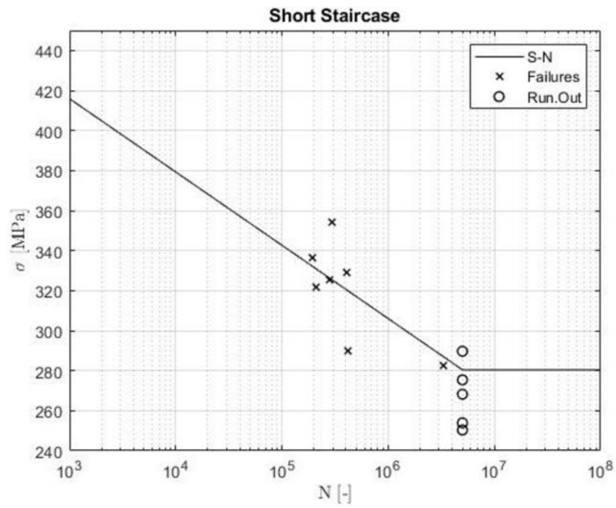


**Figure 6.** Short staircase S-N curve

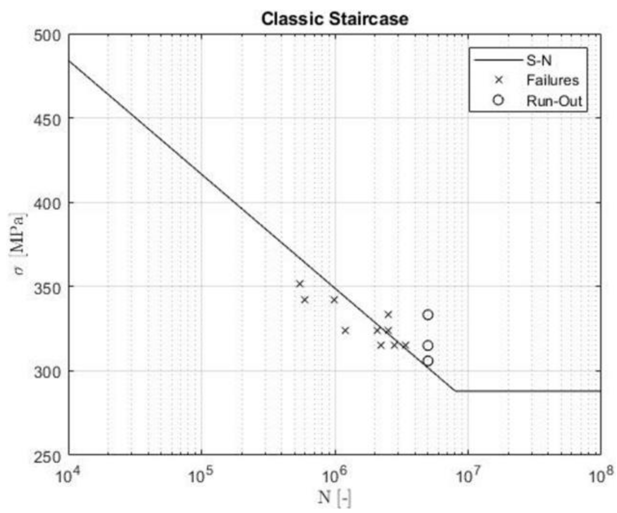


**Figure 7.** Classic staircase S-N curve

As mentioned in the previous paragraphs, a different approach for the computation of the size factor $Y_X$ was used. This particular correction coefficient was calculated implementing a new method developed by Dobler et al. [19] (Eq. (8)). Thanks to this new approach the resultant value of the size factor was set to $Y_X$=1.18, which is slightly different if considering the value suggested from the standard (=1). The last step was the one in which the admissible bending stress related to the tooth root was calculated. According to Eq. (9) values were found out at $\sigma_{Flim}$=280.44$MPa$ and $\sigma^{*}_{Flim} = 288MPa$. Figure 6 and Figure 7 display the final outputs of the experimental tests. In particular, the two S-N curves (50% failure probability) drown according to tests results are presented.

## 4. CONCLUSION

The admissible stress of the material calculated thanks to the two different statistic approaches, short and classic staircase, is $\sigma_{Flim}$=280.44$MPa$ and $\sigma^{*}_{Flim} = 288.00\ MPa$ respectively. Tests were performed on 3 different samples of the same batch, one gear for the short-case and two for the standard approach. By evaluating results, it is possible to observe a 2.5% discrepancy between the two founded values. The load increment applied in both tests (100N) was above the standard deviation for the first data distribution while for the second one it was below the suggested value. The choice of the load step cannot be chosen before tests run because the sequence of tests depends on whether a test specimen reaches rupture or the run-out condition. As discussed in previous paragraphs the main advantage of having followed the Dixon short approach was definitely the shorter time needed to perform tests and evaluate results. On the other hand, the classic approach relies on more data which do not require to introduce an additional statistic parameter. If the two founded values are compared with the one stated in literature ($\sigma_{Flim}$=280.44$MPa$) for the same steel material (39$NiCrMo$3) it is possible to say that the observation of Dobler et al. is confirmed. In practice, if the standard ISO 6336 was followed (using a value of $Y_X$=1) the resulting values of the admissible stresses result equal to $\sigma_{Flim}$=330.65$MPa$ and $\sigma^{*}_{Flim} = 339.57\ MPa$ with 17.7% and 20.8% differences respectively with the one expected. In this regard if we consider a standard 5mm module gear, that is made by the same constituent, results highlighted that the use of the alternative method for calculating the size factor leads to a 17.7% and 20.8% increment of the load carrying capacity. Moreover, it was also possible to state that outcomes of the research carried out by Dobler et al. were confirmed. It has to be noticed that several other different approaches for the calculation of the size factor are present in literature [17]. More efforts should be put into the research of this so widely used mechanical components. This fact is fully confirmed by results of the present work. A correct design phase may lead to a faster and less costly development of small sized gearboxes.

## REFERENCES


[1] Punov, P., Evtimov, T., Chiriac, R., Clenci, A., Danel, Q., Descombes, G. (2018). Progress in high performances, low emissions, and exergy recovery in internal combustion engines. Exergy for A Better Environment and Improved Sustainability 1: Fundamentals, 995-1016. https://doi.org/10.1007/978-3-319-62572-0_64

[2] American Gear Manufacturers Association. (2004). ANSI/AGMA 2001-D04, Fundamental Rating Factors and Calculation Methods for Involute Spur and Helical Gear Teeth. Alexandria, VA: American Gear Manufacturers Association.

[3] International Organization for Standardization. (2018). ISO 6336-3 ISO Stand.

[4] German Institute for Standardisation 1987 DIN 3990. Calculation of Load Capacity of Cylindrical Gears—Introduction and General Influence Factors.

[5] Gorla, C., Rosa, F., Conrado, E., Concli, F. (2017). Bending fatigue strength of case carburized and nitrided gear steels for aeronautical applications. International Journal of Applied Engineering Research, 12(21): 11306-11322.

[6] Gorla, C., Conrado, E., Rosa, F., Concli, F. (2018). Contact and bending fatigue behaviour of austempered ductile iron gears. Proceedings of the Institution of Mechanical Engineers, Part C: Journal of Mechanical Engineering Science, 232(6): 998-1008. https://doi.org/10.1177/0954406217695846

[7] Rao, S.B., McPherson, D.R. (2003). Experimental characterization of bending fatigue strength in gear teeth. Gear Technology, 20(1): 25-32.

[8] Gorla, C., Rosa, F., Concli, F., Albertini, H. (2012). Bending fatigue strength of innovative gear materials for wind turbines gearboxes: Effect of surface coatings. In ASME International Mechanical Engineering Congress and Exposition, 45233: 3141-3147. https://doi.org/10.1115/IMECE2012-86513

[9] Concli, F. (2018). Austempered Ductile Iron (ADI) for gears: Contact and bending fatigue behavior. Procedia Structural Integrity, 8: 14-23. https://doi.org/10.1016/j.prostr.2017.12.003

[10] Steutzger, M. (1997). Großeneinfluss auf die Zahnfussfestigkeit. Frankfurt, Germany.

[11] Hertter, T. (2003). Rechnerischer Festigkeitsnachweis der Ermüdungstragfähigkeit vergüteter und einsatzgehärteter Stirnräder. Doctoral dissertation, Technische Universität München.

[12] Höhn, B. R., Oster, P., Braykoff, C. (2010). Size and material influence on the tooth root, pitting, scuffing and wear load carrying capacity of fine module gears. In International Conference on Gears, Garching, pp. 1295-1307.

[13] Höhn, B.R., Oster, P. (2011). Calcolo della capacitá di carico degli ingranaggi con piccolo modulo. Organi di Trasmissione, 9: 104-112.

[14] Conrado, E., Gorla, C., Davoli, P., Boniardi, M. (2017). A comparison of bending fatigue strength of carburized and nitrided gears for industrial applications. Engineering Failure Analysis, 78: 41-54. https://doi.org/10.1016/j.engfailanal.2017.03.006

[15] Gorla, C., Rosa, F., Conrado, E., Albertini, H. (2014). Bending and contact fatigue strength of innovative steels for large gears. Proceedings of the Institution of Mechanical Engineers, Part C: Journal of Mechanical Engineering Science, 228(14): 2469-2482. https://doi.org/10.1177/0954406213519614

[16] Bonaiti, L., Concli, F., Gorla, C., Rosa, F. (2019). Bending fatigue behaviour of 17-4 PH gears produced via selective laser melting. Procedia Structural Integrity,

24: 764-774. https://doi.org/10.1016/j.prostr.2020.02.068

[17] Concli, F. (2021). Tooth root bending strength of gears: Dimensional effect for small gears having a module below 5 mm. Applied Sciences, 11(5): 2416. https://doi.org/10.3390/app11052416

[18] Concli, F., Fraccaroli, L. (2021). Bending fatigue strength of small size 2 mm module gears. WIT Transactions on Engineering Sciences, 133: 39-46.

[19] Dobler, D.I.A., Hergesell, I.M., Stahl, I.K. (2016). Increased tooth bending strength and pitting load capacity of fine-module gears. Gear Technol, 33(7): 48-53.

[20] Rettig, H. (1987). Ermittlung von Zahnfußfestigkeitskennwerten auf Verspannungsprüfständen und Pulsatoren-Vergleich der Prüfverfahren und der gewonnenen Kennwerte. antriebstechnik, 26(1): 51-55.

[21] Stahl, K. (1999). Lebensdauerstatistik: Abschlussbericht: Forschungsvorhaben Nr. 304. FVA.

[22] Dixon, W.J. (1965). The up-and-down method for small samples. Journal of the American Statistical Association, 60(312): 967-978.

[23] Concli, F., Fraccaroli, L., Nalli, F., Cortese, L. (2021). High and low-cycle-fatigue properties of 17–4 PH manufactured via selective laser melting in as-built, machined and hipped conditions. Progress in Additive Manufacturing, 7: 99-109. https://doi.org/10.1007/s40964-021-00217-y

[24] Yin, G.Q., Kang, X., Zhao, G.P. (2017). Fatigue properties of the ultra-high strength steel TM210A. Materials, 10(9): 1057. https://doi.org/10.3390/ma10091057

[25] Concli, F., Gilioli, A., Nalli, F. (2021) Experimental–numerical assessment of ductile failure of Additive Manufacturing selective laser melting reticular structures made of Al A357. Proceedings of the Institution of Mechanical Engineers, Part C: Journal of Mechanical Engineering Science, 235 (10): 1909-1916. https://doi.org/10.1177/0954406219832333

[26] Gasparini, G., Mariani, U., Gorla, C., Filippini, M., Rosa, F. (2008). Bending fatigue tests of helicopter case carburized gears: Influence of material, design and manufacturing parameters. In American Gear Manufacturers Association (AGMA) Fall Technical Meeting, pp. 131-142.

[27] Bonaiti, L., Bayoumi, A., Concli, F., Rosa, F., Gorla, C. (2021). Gear root bending strength: A comparison between single tooth bending fatigue tests and meshing gears. Journal of Mechanical Design, Transactions of ASME, 143(10): 103402. https://doi.org/10.1115/1.4050560

[28] German Institute for Standardisation. DIN 4778; German Institute for Standardisation: Berlin, Germany, 1990.

[29] International Organization for Standardization 2003 ISO 6336-5 ISO Stand. 50.